Ras Inhibition in Glioblastoma Down-regulates Hypoxia-Inducible Factor-1α, Causing Glycolysis Shutdown and Cell Death

Roy Blum,[1] Jasmine Jacob-Hirsch,[3] Ninette Amariglio,[3] Gideon Rechavi,[2,3] and Yoel Kloog[1]

[1]Department of Neurobiochemistry, George S. Wise Faculty of Life Sciences and [2]Sackler School of Medicine, Tel-Aviv University, Tel-Aviv, Israel and [3]Department of Pediatric Hematology-Oncology, Safra Children's Hospital, Sheba Medical Center, Tel Hashomer, Israel

Abstract

Active Ras and phosphatidylinositol-3-kinase–dependent pathways contribute to the malignant phenotype of glioblastoma multiformes (GBM). Here we show that the Ras inhibitor *trans*-farnesylthiosalicylic acid (FTS) exhibits profound antioncogenic effects in U87 GBM cells. FTS inhibited active Ras and attenuated Ras signaling to extracellular signal-regulated kinase, phosphatidylinositol-3-kinase, and Akt. Concomitantly, hypoxia-inducible factor 1α (HIF-1α) disappeared, expressionof key glycolysis pathway enzymes and of other HIF-1α–regulated genes (including vascular endothelial growth factor and the Glut-1 glucose transporter) was down-regulated, and glycolysis was halted. This led to a dramatic reduction in ATP, resulting in a severe energy crisis. In addition, the expression of E2F-regulated genes was down-regulated in the FTS-treated cells. Consequently, U87 cell growth was arrested and the cells died. These results show that FTS is a potent down-regulator of HIF-1α and might therefore block invasiveness, survival, and angiogenesis in GBM. (Cancer Res 2005; 65(3): 999-1006)

Introduction

Glioblastoma multiformes (GBM), the most common subtypes of malignant brain tumors in adult humans (1, 2), are highly invasive, angiogenic, and incurable. Chromosomal abnormalities commonly found in gliomas include those that disrupt cell cycle arrest and death pathways and those that promote survival under hypoxic conditions (1–3). GBMs frequently show loss of the phosphatase PTEN (4, 5). PTEN hydrolyzes phosphatidylinositol 3,4,5-triphosphate, the phospholipid product of phosphatidylinositol-3-OH kinase (PI3-K), which regulates inter alia the protein kinases phosphoinositide-dependent kinase and Akt (6). Phosphoinositide-dependent kinase together with phosphatidylinositol 3,4,5-triphosphate activates Akt and thereby induces multiple effects including enhancement of metabolism through the action of Akt on glycogen synthase-3β (7). Other common alterations in GBMs activate signal-transduction pathways downstream of receptor tyrosine kinases (1, 8). These alterations include overexpression of platelet-derived growth factor (PDGF), fibroblast growth factor 2, vascular endothelial growth factor (VEGF), and amplification of or activating mutations in the epidermal growth factor receptor (*EGFR*) gene (9).

Cell culture experiments with glioma cell lines have provided persuasive evidence that various RTKs activate several common pathways and, in particular, those that lead to activation of Akt and Ras. Receptor-mediated Ras activation, which facilitates exchange of GDP for GTP (10), and Ras activation by oncogenic mutation are common in human tumors and contribute to the development and maintenance of the malignant phenotype (11). For example, the active Ras-GTP protein, through its downstream effectors including Raf, PI3-K, and Ral-guanine nucleotide exchange factors, promotes cell cycle progression, survival, and migration (10, 12). Although oncogenic mutations that affect Ras are not prevalent in human gliomas, recent studies revealed the abundant presence of Ras-GTP in these tumors (13). Thus, receptor-mediated activation of Ras signaling might be required for the induction, progression, and maintenance of gliomas. Consistent with this suggestion, expression of dominant-negative Ras in the glioma cell line U373 results in inhibition of Ras signaling to the Raf/MEK/ERK and attenuation of cell growth (13). Attempts have been made to block Ras or Ras-dependent functions in GBM cells using farnesyl transferase inhibitors (14). However, knowledge of the direct effect of Ras inhibitors on human GBM cells is still limited. In the present study, we used the potent Ras inhibitor S-trans, *trans*-farnesylthiosalicylic acid (FTS), which affects directly the membrane-bound Ras protein (15). Our results show that FTS induces growth arrest and cell death in U87 GBM.

Materials and Methods

Cell lines and Reagents. Cell lines (U87, U373, DBTRG-05MG (20/20), and LN229) were kindly supplied by Eric C. Holland (Memorial Sloan-Kettering Cancer Center, New York, NY). FTS was prepared as previously described in detail (16). Mouse anti-pan-Ras antibody and isoform-specific mouse anti-Ras antibodies were from Calbiochem (La Jolla, CA); mouse anti-phospho-ERK antibody and mouse anti-β-tubulin antibody (AK-15) were from Sigma-Aldrich (St. Louis, MO); rabbit anti-phospho-ERK1/2 antibody and goat anti-aldolase c were from Santa Cruz Biotechnology (Santa Cruz, CA); rabbit anti-phospho-Akt (Ser^{473}; 4E2) antibody and rabbit anti-phospho-mTOR (Ser^{2448}) were from Cell Signaling (Beverly, MA); rabbit anti-PI3-K p85 antibody was from Upstate Biotechnology (Lake Placid, NY); mouse anti–hypoxia-inducible factor 1α (HIF-1α) antibody was from BD Transduction Laboratories (San Jose, CA); peroxidase-goat antimouse immunoglobulin G, peroxidase-goat antirabbit immunoglobulin G and peroxidase-donkey anti-goat immunoglobulin G were from Jackson ImmunoResearch Laboratories (West Grove, PA); anti-VEGF antibody was a gift from G. Neufeld (Technion, Haifa, Israel); rabbit anti-PFKFB4 was from Abgent (San Diego, CA); goat anti–lactate dehydrogenase antibody was from abcam (Cancun, Mexico). Carbobenzoxy-L-leucyl-L-leucinalZ-LLL-CHO (MG132) was from Calbiochem (La Jolla, CA).

Cell Culture and Cell Proliferation Assays. Cells were grown at 37°C in DMEM containing 5% FCS, 100 μg/mL streptomycin, and 100 units/mL penicillin and maintained in a humidified atmosphere of 95% air/5% CO_2 (normoxia) or of low oxygen pressure (1% O_2) where indicated. Cells were plated at a density of 5,000 cells per well in 24-well plates for direct cell-count assays, in 96-well plates for cell-proliferation assays [bromodeoxyuridine (BrdUrd) labeling and detection kit III, Roche Molecular Biochemicals,

Note: Y. Kloog is the incumbent of the Jack H. Skirball Chair for Applied Neurobiology. G. Rechavi is the incumbent of the Djerassi Chair in Oncology.

Supplementary data for this available at Cancer Research Online (http://cancerres.aacrjournals.org).

Requests for reprints: Yoel Kloog, Department of Neurobiochemistry, George S. Wise Faculty of Life Sciences, Tel-Aviv University, 69978 Tel-Aviv, Israel. Phone: 972-3-640-9699; Fax: 972-3-640-7643; E-mail: yoelk@tauex.tau.ac.il.

Mannheim, Germany], or at a density of 1.5×10^6 cells in 10-cm dishes for all other assays including fluorescence-activated cell-sorting (FACS) analysis of propidium iodide (BDH, Poole, United Kingdom)–stained cells. The cells were treated 24 hours after plating or 12 hours after serum starvation, with different concentrations of FTS or with the vehicle (0.1% DMSO). All assays were done in triplicate or quadruplicate. Data were expressed as means ± SD. Statistical significance was determined by an unpaired Student's *t* test.

Immunoblotting, Ras-GTP, and PI3-K Assays. To determine the effects of FTS on Ras and its downstream signals on HIF-1α, VEGF, aldolase c, lactate dehydrogenase, and PFKFB4 we used lysates of cells pretreated with 70 μmol/L FTS for 24 hours as described above and did Western immunoblotting analysis or Ras-GTP and PI3-K assays (17). Protein bands were visualized by enhanced chemiluminescence (ECL, Amersham Biosciences AB, Buckinghamshire, United Kingdom) and quantified as detailed (17). Ras-GTP was determined by the glutathione *S*-transferase-Ras binding domain of Raf (RBD) pull-down assay as previously described (17). PI3-K activity was determined essentially as detailed earlier (17). All biochemical and immunoblotting assays were repeated at least thrice. Data are presented as means ± SD.

Immunocytochemistry. U87 glioblastoma cells were cultured to approximately 80% confluence on glass coverslips in six-well plates and incubated with 70 μmol/L FTS or the vehicle (0.1% DMSO) for 48 hours in hypoxic conditions (1% O_2). The cells were fixed, permeabilized, and labeled with HIF-1α antibody and Red Cy3–conjugated donkey anti-mouse as detailed earlier (18). The cells were then imaged with a fluorescence microscope IX70 (Olympus America, Inc., Melville, NY) with a 1.40 numerical aperture, 63× objective, and Cy3 filter set, using the 4.0.4 SpotAdvanced imaging software.

Measurements of pH and ATP. The pH of the culture medium and the free ATP in the cells was measured to assess the effects of FTS on the end products of glycolysis. U87 cells (triplicate samples) were treated with 70 μmol/L FTS or with the vehicle (0.1% DMSO), as described above, for the indicated periods. Media were collected and the pH was immediately determined. A constant light signal luciferase assay (ATP bioluminescence assay kit CLSII, Boehringer Mannheim Biochemicals, Mannheim, Germany) was used to determine the cellular content of free ATP according to the manufacturer's instructions.

Gene Expression Profiling. All experiments were done using Affymetrix Human Genome Focus oligonucleotide arrays (Santa Clara, CA). The effect of FTS on gene expression in U87 cells was determined 24 and 48 hours after treatment with FTS (70 μmol/L) or vehicle (a single microarray for each condition). Zero time incubation was included. Total RNA from each sample was used to prepare biotinylated target RNA that was used to generate cRNA as detailed http://bioinf.picr.man.ac.uk/mbcf/downloads/GeneChip_Target_Prep_Protocol-CR-UK_v3.pdf). Spike controls were added to 15 μg of fragmented cRNA before overnight hybridization. Arrays were then processed and scanned on an Affymetrix GeneChip scanner as detailed at the above Web site. The quality and amount of total RNA were analyzed using an agarose gel. After scanning, array images were assessed visually to confirm scanner alignment and the absence of significant bubbles or scratches on the chip surface. Ratios of 3′/5′ for glyceraldehyde-3-phosphate dehydrogenase and β-actin were confirmed to be within acceptable limits (0.91-1.13 and 0.95-1.39, respectively) and BioB spike controls were found to be present on all the arrays, with BioC, BioD, and CreX also present with increasing intensity. When scaled to a target intensity of 150 (using Affymetrix Microarray Suite 5.0 array analysis software), scaling factors for all arrays were found to be within acceptable limits (0.56-1.2), as were the background, *Q* values, and mean intensities. Details of quality control measures are recorded in the supplement (see quality control table in http://eng.sheba.co.il/genomics).

Analysis of Gene Expression Data. Genes were analyzed using the MAS 5 algorithm (see pivot data in supplement http://eng.sheba.co.il/genomics). A list of 5,054 probe sets, or "valid genes," was obtained, representing probe sets with signals higher than 20 and detected as present in at least one sample (see valid genes in http://eng.sheba.co.il/genomics). A comparison of FTS-treated cell samples with untreated cell samples yielded a list of 1,212 "active genes" (see active genes in http://eng.sheba.co.il/genomics), representing genes whose expression was increased by at least 2-fold (log ratio ≥1), detected as an "increase" or a "marginal increase", or genes whose expression was decreased by at least 2-fold (log ratio ≤−1), detected as a "decrease" or a "marginal decrease" at least at one time point. Hierarchical clustering was done using Eisen clustering and visualization tools (ref. 19; http://rana.lbl.gov/EisenSoftware.htm). Genes were classified into functional groups using the GO annotation tool (ref. 20; http://apps1.niaid.nih.gov/David/upload.asp). Overabundance was calculated using EASE software (21).

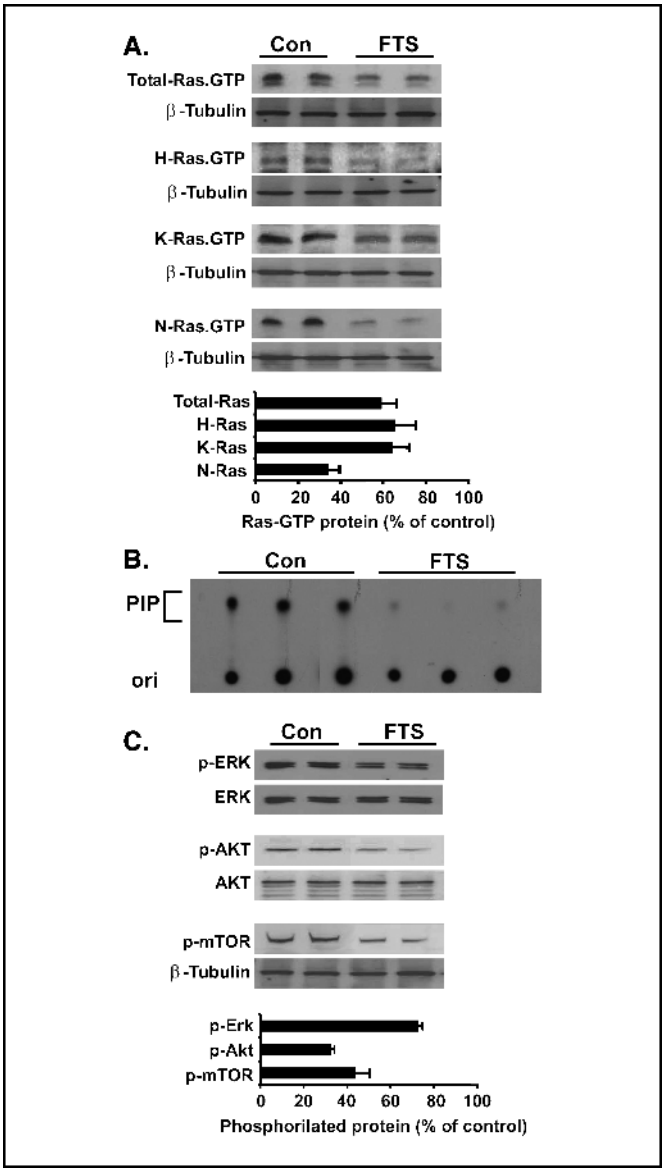

Figure 1. FTS inhibits active Ras and Ras signaling in U87 GBM cells. Cells were treated with 70 μmol/L FTS for 24 hours, then lysed and subjected to the specified assays. *A,* FTS decreases the amounts of all three active Ras isoforms in U87 cells. Lysates were subjected to the Ras-GTP RBD pull-down assay followed by immunoblotting with the indicated anti-Ras antibodies (see Materials and Methods). Samples of total cell lysates were also immunoblotted with anti-β-tubulin antibody. Immunoblots of a typical experiment and densitometric analysis. *Bottom, columns,* mean (n = 3); *bars,* SD. *B,* FTS inhibits PI3-K activity. Lysates were subjected to immunoprecipitation with anti-PI3-K p85 antibody and PI3-K activity was then determined. The ^{32}P-labeled lipid products separated by thin-layer chromatography were visualized by overnight exposure to an X-ray film. The phosphatidylinositol-3-phosphate (*PIP*) spots were then subjected to quantitative densitometry. Results of a representative experiment done in triplicate. *Con,* control. *C,* FTS reduces phospho-ERK, phospho-Akt, and phospho-mTOR. Cell lysates were immunoblotted with anti-phospho-ERK, anti-ERK, anti-phospho-Akt, anti-Akt, anti-phospho-mTOR, or anti-β-tubulin antibodies (see Materials and Methods). Typical duplicate immunoblots and densitometric analysis. *Bottom, columns,* mean (n = 3); *bars,* SD.

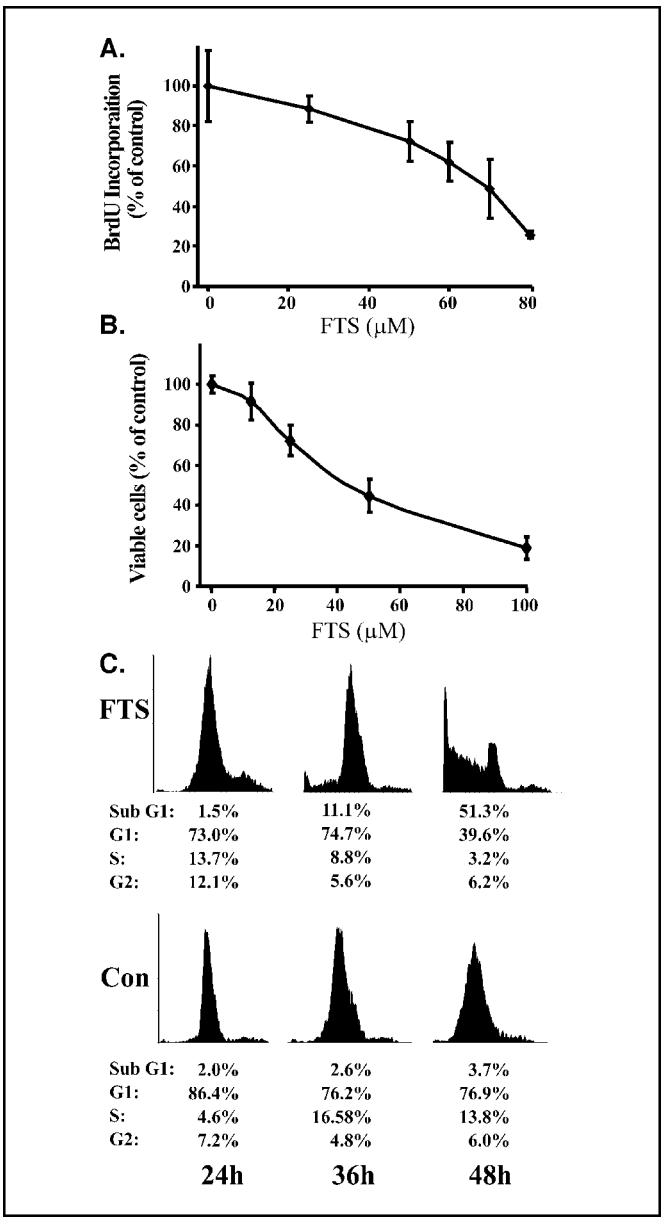

Figure 2. FTS inhibits U87 cell growth and induces cell death. *A,* dose-dependent inhibition of BrdUrd incorporation into DNA by FTS. Cells were starved of serum for 12 hours, then stimulated by 5% FCS in the absence and in the presence of the indicated concentrations of FTS and subjected to the BrdUrd assay 24 hours later. Levels of BrdUrd incorporation in the controls (100%) were 0.5 ± 0.09 $OD_{(370\text{-}492\ nm)}$. *Points,* mean of data expressed in terms of BrdUrd incorporation into DNA in FTS-treated cells as a percentage of control (n = 4); *bars,* SD. *B,* FTS inhibits U87 cell growth. The cells were incubated for 5 days in the absence and in the presence of the indicated concentrations of FTS, then detached from the plates and counted. The number of cells in the control was (4.5 ± 0.2) × 10^4. The numbers of cells in FTS-treated samples, calculated as a percentage of the total number of cells in the control, are plotted against the concentration of FTS. *Points, mean* (n = 3); *bars,* SD. *C,* FACS analysis of FTS-treated U87 cells. Cells were treated with 70 μmol/L FTS for the indicated periods and then subjected to FACS analysis (see Materials and Methods). Cell cycle distribution of the control and of the FTS-treated cells was monitored by flow cytometry. Data from one of three experiments with similar results. *Con,* control.

Functional classifications with an EASE score lower than 0.05 were marked as overabundant.

Real-time PCR analysis. Extracts of total RNA (1 μg) from cells treated for 48 hours with FTS (70 μmol/L) or vehicle (control) were reverse-transcribed in a total volume of 20 μL using the iSCRIPT cDNA kit (Bio-Rad). The cDNA samples were then used for real-time PCR (Syber Green PCR kit, Roche). The PCR conditions and the primers used for *PFKFB3*, *Glut-1* (*SLC2A1*), *PDGFRA*, and *VEGFC* genes and for the housekeeping genes *GAPDH* and *HMBS* are detailed in the supplement (Real-time PCR Table, http://eng.sheba.co.il/genomics).

Results

Ras Inhibition in U87 Cells Results in Growth Arrest and Cell Death. U87 cells exhibited significant amounts of activated (GTP-bound) H-Ras, K-Ras and N-Ras (Fig. 1*A*). The Ras inhibitor FTS reduced the total amount of Ras-GTP as well as the amounts of each of the active Ras isoforms within 24 hours (Fig. 1*A*). The extent of inhibition, expressed as a percentage (mean ± SD, n = 3) of the activity in untreated controls was 41.5 ± 6.8% (P < 0.001), 35.1 ± 9.3% (P < 0.003), 36.2 ± 7.1% (P < 0.007), and 66.5% ± 5.9 (P < 0.03) for total Ras-GTP, H-Ras-GTP, K-Ras-GTP, and N-Ras-GTP, respectively (Fig. 1*A*).

Figure 1*C* shows that treatment of U87 cells with FTS for 24 hours resulted in a significant reduction in active phospho-ERK (by 27.6 ± 0.5% relative to controls, P < 0.0007; n = 3). Total ERK was not affected by FTS. The inhibitor had an even stronger effect on the Ras effector PI3-K, reducing its activity by 74 ± 0.6% (P <0.005;

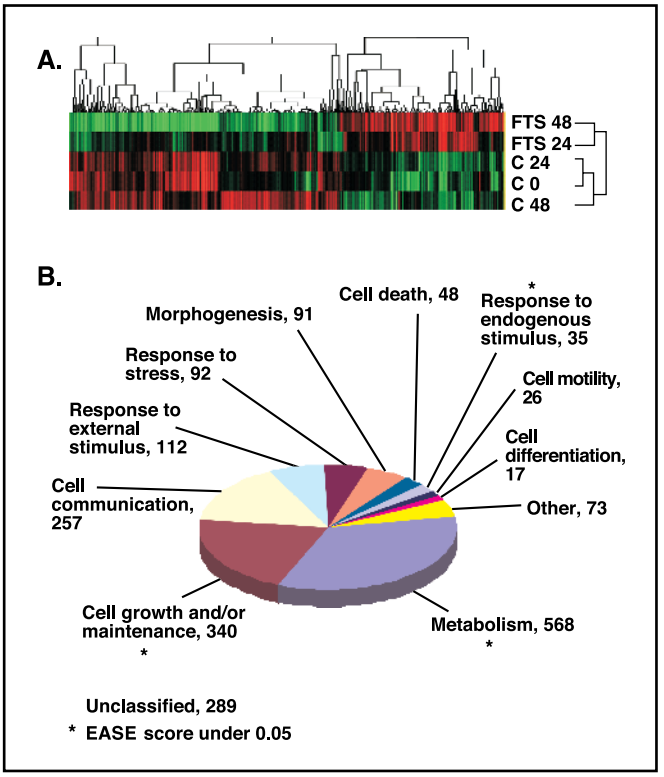

Figure 3. Comparative gene expression profiles of FTS-treated and untreated U87 cells. Samples of cells at the zero time point (*C0*) and of cells treated for 24 (*C24*) or 48 hours (*C48*) with vehicle (*F24*) or FTS (*F48*) were processed for microarray gene analysis (see Materials and Methods). *A,* results of unsupervised hierarchical clustering of 5,054 valid genes summarized in a dendrogram. *Red,* high relative expression; *green,* low relative expression. *Columns,* samples; *rows,* genes. Note that the clearest distinction between groups is that of the samples of treated and untreated cells. *B,* functional clustering analysis. The data obtained as described in *A* were filtered using cutoff values of 2-fold differences and above (defined as active genes) and subjected to functional clustering analysis (see Materials and Methods). Results of the analysis. *, overabundant groups, EASE score below 0.05.

$n = 3$; Fig. 1*B*). Active phospho-Akt and phospho-mTOR (phospho-mammalian target of rapamycin), enzymes downstream of PI3-K, were also significantly reduced within 24 hours (67.7 ± 0.3% and 56.6 ± 6.9% reduction, respectively, relative to controls, $P < 0.006$; $n = 3$; Fig. 1*C*). Taken together, these experiments showed that FTS inhibited Ras and its downstream signals in U87 cells.

Next we examined the effect of FTS on U87 cell proliferation. Serum-stimulated BrdUrd incorporation into DNA was inhibited by FTS, with 50% inhibition occurring at 70 μmol/L FTS (Fig. 2*A*). Counting of cells grown for 5 days in the presence of FTS showed that the drug induced a dose-dependent decrease in cell number (with 50% decrease at 50 μM FTS; Fig. 2*B*). This decrease was attributable not only to inhibition of proliferation; FACS analysis carried out 48 hours after FTS treatment showed that the drug induced a time-dependent increase in the sub-G_1 cell population (Fig. 2*C*) indicating that the observed decrease in cell number is in part a reflection of cell death (51% of the cells were not viable after 48 hours of FTS treatment). This finding suggests that the Ras inhibitor affected a multitude of Ras-dependent pathways that control cell growth and cell death or survival.

Gene Array Profiling of FTS-Treated U87 Human GBM. In light of the complex phenotypic changes that apparently occur in U87 cells after treatment with the Ras inhibitor, we opted for gene expression analysis. We incubated U87 cells with 70 μmol/L FTS for 24 or 48 hours and extracted RNA for gene expression analysis, using the Affymetrix Human Genome Focus Array (8,500 sequences). The zero time point of untreated cells was taken as a reference point. This yielded a list of 5,054 "valid genes" (see supplement,

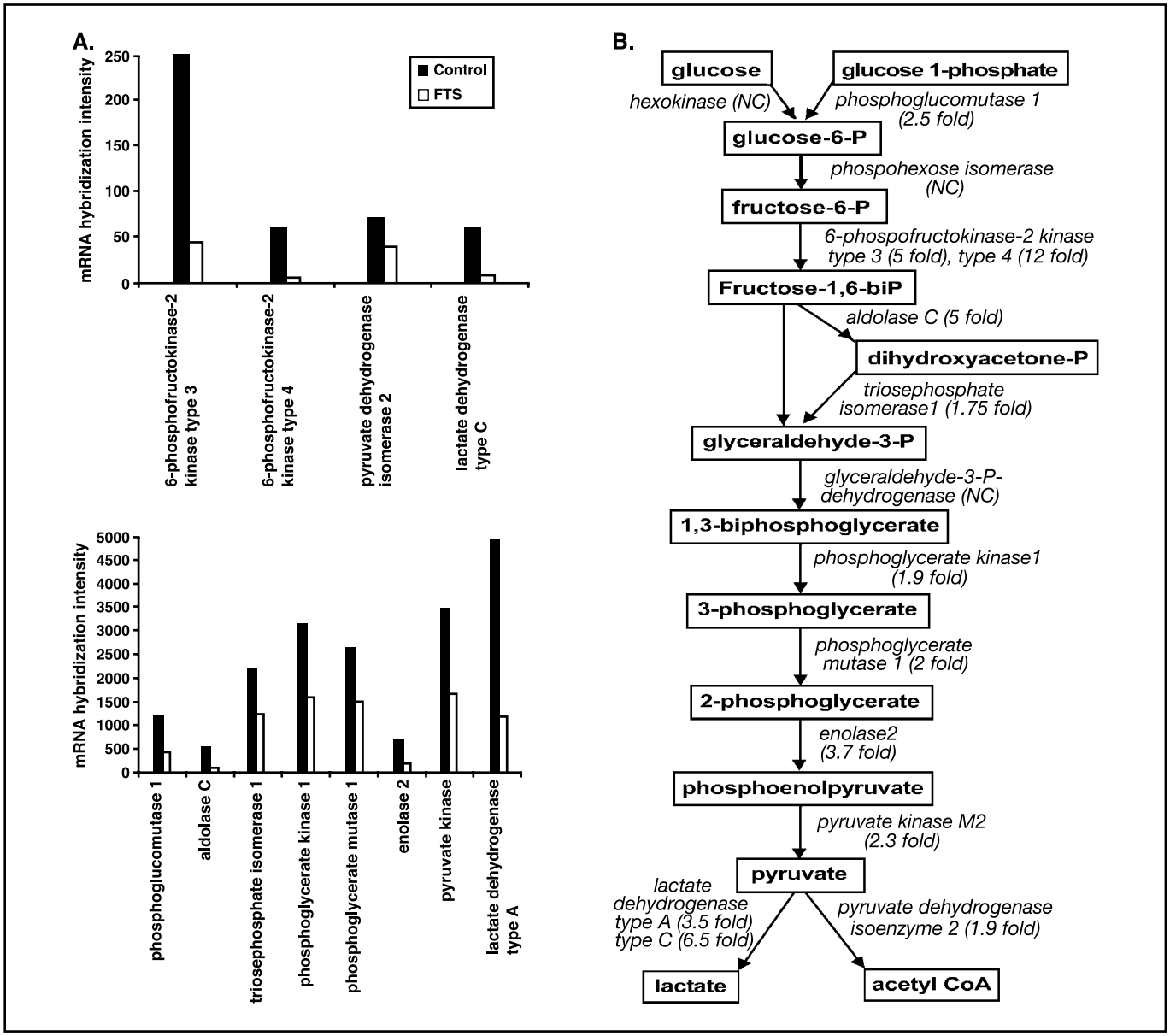

Figure 4. FTS induces decreased expression of glycolysis pathway genes in U87 cells. *A,* levels of mRNA hybridization intensity for control and FTS-treated cells (48 hours). Data from control and FTS-treated cells were evaluated as described in Fig. 3. *B,* scheme of the glycolysis pathway including the fold decreases in the expression of genes encoding the relevant enzymes, relative to control. *NC,* no change.

http://eng.sheba.co.il/genomics). Further analysis of the data, using an unsupervised average-linkage hierarchical clustering analysis, showed that all three control samples (vehicle-treated cells at 0, 24, and 48 h) were grouped together in one branch and the samples of FTS-treated cells (drug treatments at 24 and 48 hours) were grouped together in a separate branch (Fig. 3*A*). This indicates that the major factor affecting clustering was the FTS treatment.

To focus on the most prominent FTS-induced changes in gene expression we compared samples of treated and untreated cells, using a 2-fold difference as a cutoff value. This generated a list of 1,212 active genes (see supplement, http://eng.sheba.co.il/genomics), for which we did functional analysis using the GO annotation tool (20). The analysis (Fig. 3*B*) pointed to three major groups of genes whose expression was altered by FTS treatment: (*a*) genes that participate in metabolism; (*b*) genes that participate in cell growth; and (*c*) genes that participate in cell communication. Overabundance of specific functional groups was determined using the expression analysis systematic explorer (EASE) software tool (21). The EASE score analysis indicated that genes in the first two groups, namely, in the group of genes that are involved in cell growth ($P \leq 0.00217$) and in the group of genes that are involved in metabolism ($P \leq 0.0000903$) were overabundant in the FTS-treated cells.

Analysis of genes in the category of cell growth indicated dramatic changes in the expression of enzymes that participate in cell cycle, cell cycle arrest, cell cycle checkpoint, cell differentiation, cell proliferation, chromatin modification, DNA metabolism, DNA repair, and mitotic pathways (see valid genes in supplement, http://eng.sheba.co.il/genomics). Thus, for example, we observed a decrease in expression of the following genes (the fold decrease in each case is given in parentheses): *cyclin E2* (4.6), *cyclin A2* (7.5), *cyclin B2* (6.5), *Orc1L* (19.7), *Mcm5* (9.2), *CDC2* (24), and *POLE* (8). Although these results need to be validated, they clearly are consistent with the observed FTS-induced inhibition of U87 cell proliferation (Fig. 2*A* and *B*). In addition, they are in accord with the known regulation of the cell cycle by active Ras and Ras-dependent pathways (22).

FTS Decreases the Expression of Genes Regulated by HIF-1α. Examination of the FTS-induced alterations in genes that participate in metabolism suggested that 12 genes of the ubiquitously expressed glycolytic pathway were transcriptionally down-regulated by FTS (see mRNA hybridization intensity, Fig. 4*A*). The fold decreases in the expression of genes encoding the relevant enzymes, relative to control, are indicated in Fig. 4*B*. The decrease was most prominent in phosphofructokinase (PFKFB4 and PFKFB3), the rate-limiting glycolytic enzyme. Real-time PCR analysis showed that FTS reduced the expression of the *PFKFB3* gene by a factor of 2.7 ± 0.006. The above-mentioned decrease in the expression of genes of the glycolytic pathway was also manifested at the protein level. This is shown by the observed decrease in the amounts of three key glycolytic enzymes (Fig. 5*A*).

Because the expression of most of the enzymes of the glycolytic pathway is controlled by the transcription factor HIF-1α (23, 24) it seemed reasonable to assume that FTS affected HIF-1α, even though the gene-profiling data did not indicate a significant decrease in *HIF-1α* gene expression. This latter finding was expected, because HIF-1α protein levels are controlled mainly via posttranslational degradation. Consistent with this possibility, we found that the expression of more than 20 other genes controlled by HIF-1α was down-regulated by FTS (see Table 1). Notably, this list includes the genes encoding VEGFC (25), transforming growth factor α, and PDGFRA (important for GBM cell motility; ref. 26), DEC-1 (important for adaptation to hypoxia, ref. 27), and the major glucose transporter Glut-1 (28). Real-time PCR validated the FTS-induced decrease in the expression of *Glut-1* (6.5 ± 0.017), *PDGFRA* (11.5 ± 0.007), and *VEGFC* (3.0 ± 0.03). In addition, immunoblotting analysis with anti-VEGF antibody showed that VEGF protein was down-regulated as well (Fig. 5*A*).

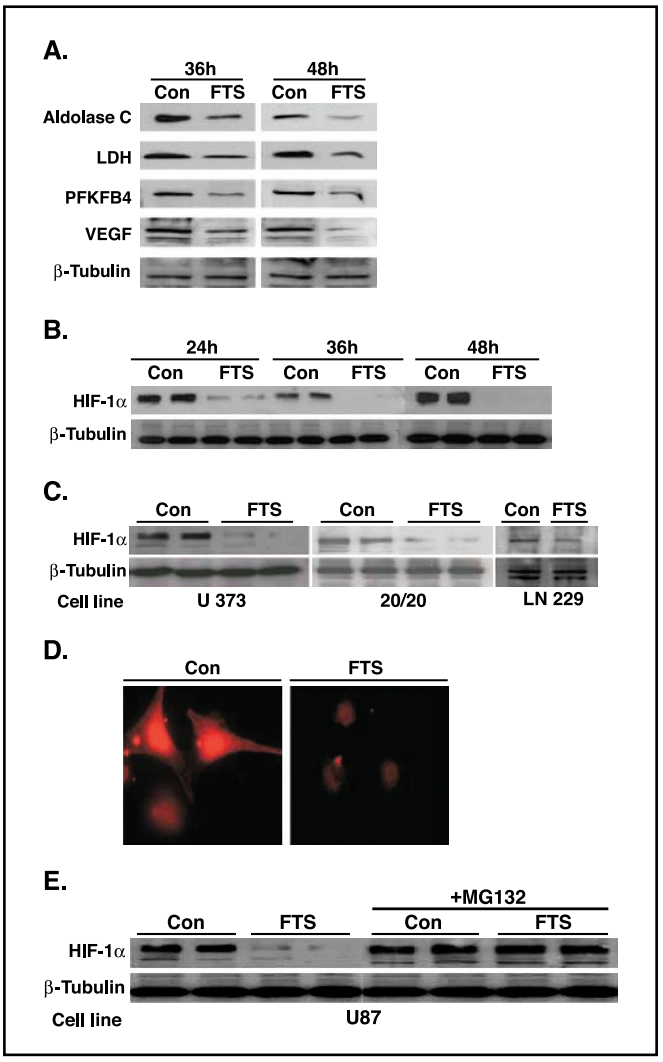

Figure 5. FTS down-regulates HIF-1α and HIF-1α-regulated proteins in GBM cells. GBM cell lines were incubated under hypoxia (1% O_2) for the indicated periods with 70 μmol/L FTS and then processed for the determination of HIF-1α, aldolase c, lactate dehydrogenase, PFKFB4, or VEGF by immunoblotting. Samples of total cell lysates were also immunoblotted with anti-β-tubulin antibody. Results of representative experiments, each done at least thrice. *A,* Control and FTS-treated U87 cells were subjected to immunoblotting for the determination of the indicated glycolytic enzymes or of VEGF. *B,* control and FTS-treated U87 cells were subjected to immunoblotting for the determination of HIF-1α. *C,* GBM cells of the lines U373, 20/20, and LN229 were grown with or without FTS for 48 hours and subjected to immunoblotting for the determination of HIF-1α. *D,* U87 cells were grown on coverslips as detailed in *A* for 48 hours then labeled with HIF-1α antibody followed by incubation with Cy3-conjugated donkey anti-mouse secondary antibody. The cells were then visualized under fluorescence microscope (×63 objective). Typical fluorescence images. *E,* U87 Cells were grown for 48 hours in the absence or presence of 5 μmol/L MG132 and subjected to immunoblotting for the determination of HIF-1α. *Con,* control.

FTS Induces Disappearance of HIF-1α Protein with Resulting Blockage of Glycolysis. Next, we examined by immunoblotting the effect of FTS on the cellular levels of HIF-1α protein. U87 cells

Table 1. Summary of HIF-1α–inducible genes whose expression was decreased

Gene name	Title	Fold decrease
PLOD	Procollagen-lysine	3
PLOD2	Procollagen-lysine 2	6.5
TGFA	Transforming growth factor, α	2.5
SLC2A1/Glut-1	Glucose transporter, member 1	3.7
BNIP3	BCL2/adenovirus E1B interacting protein 3	4
P4HA1	Proline 4-hydroxylase α polypeptide 1	8
PLAU/u-PA	Plasminogen activator, urokinase	2.5
PLAT/t-PA	Plasminogen activator, tissue	6.1
Serpin31/PA-1	Serine proteinase inhibitor, member 1	1.9
CDKN1B/P27KKI	Cyclin-dependent kinase inhibitor 1B	2
COL5A1	Collagen, type V, α 1	3.2
COL5A2	Collagen, type V, α 2	13
DEC1/BHLHB2	Basic helix-loop-helix domain containing, class	7
TGM2	Transglutaminase 2	4.9
ADM	Adrenomedullin	3.2
STC1	Stanniocalcin 1	9.8
AK3	Adenylate kinase 3	3
CA9	Carbonic anhydrase IX	137
PDGFRB	Platelet-derived growth factor receptor, polypeptide	9.2
PDGFRA	Platelet-derived growth factor receptor, α polypeptide	32
HDAC1	Histone deacetylase 1	2.3
VEGFC	Vascular endothelial growth factor C	2.1
CITED/P35SRJ	Cbp/p300-interacting transactivator 2	9.8

were grown in the presence or absence of 70 μmol/L FTS for various periods under hypoxia (1%), a condition that stabilizes HIF-1α (29). We found that FTS induced a dramatic decrease in HIF-1α within 24 hours (Fig. 5*B*). After 48 hours or 72 hours of treatment HIF-1α was almost undetectable, with levels lower than 5% of controls ($P < 0.005$). Similar results were obtained with three other GBM cell lines, namely, U373, 20/20, and LN229 (Fig. 5*C*). Immunofluorescence analysis confirmed these results; FTS treatment caused a complete disappearance of HIF-1α from the U87cells nuclei with no accumulation of the protein in the cytosol (Fig. 5*D*). The FTS-induced down-regulation of HIF-1α protein could be associated with a mechanism in which the inhibition of Akt (Fig. 1) promoted proteasomal degradation of HIF-1α as was shown previously (30). Consistent with this possibility we found that the proteasome inhibitor MG132 blocked the FTS-induced disappearance of HIF-1α (Fig. 5*E*).

These results prompted us to examine the effect of the Ras inhibitor on the principal end products of glycolysis. First, we determined the cellular content of ATP. U87 cells were treated with 70 μmol/L FTS and assayed 24, 48, and 72 hours later. All assays were normalized to equal amounts of cellular protein. ATP showed a time-dependent decrease, reaching a level corresponding to 20% of that in control cells at 72 hours (Fig. 6*A*). Next we determined the acidity of the growth medium, caused primarily by lactate, another glycolytic end product. Treatment with FTS diminished acidity, consistent with inhibition of lactate accumulation (Fig. 6*B*). Thus, the pH of the medium of the treated cells was significantly higher than that of controls (Fig. 6*B*). It should be noted that the time-dependent reduction in pH of the control cells did not result from the presence of more cells. Under the experimental conditions used and at the time points of measurement, cell numbers in the FTS-treated and control preparations were similar.

Discussion

Chronically active Ras and PI3-K, common in most GBMs, disrupt cell cycle arrest, facilitate cell migration, enhance GBM cell survival (31), and promote angiogenesis (32). We showed here that the Ras inhibitor FTS, which caused a marked decrease in active Ras, inhibited Ras signals to ERK, PI3-K, and Akt (Fig. 1). Concomitantly, HIF-1α protein disappeared (Fig. 5), expression of key enzymes of the glycolysis pathway was down-regulated (Fig. 4), and glycolysis

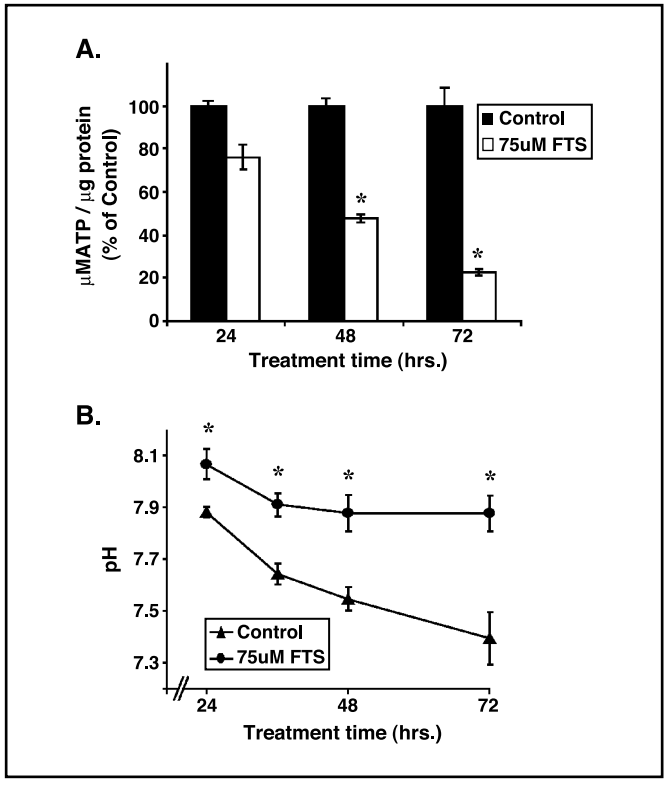

Figure 6. FTS decreases ATP and reduces acidity in U87 cells. Cells were grown under hypoxia (1% O_2) for the indicated periods and then processed for ATP determination by the bioluminescence assay as detailed under Materials and Methods (*A*). At each time point, the pH of the media was determined as well (*B*). *Columns* or *points,* mean ($n = 4$); *bars,* SD. *, $P < 0.05$, control versus FTS; *t* test.

was halted (Fig. 6). This led to a severe energy crisis in which ATP was dramatically reduced (Fig. 6). In addition, expression of E2F-regulated genes, required for cell cycle progression, was down-regulated in the FTS-treated cells (Fig. 3). Consequently, U87 cell growth was arrested and the cells died (Fig. 2).

Our data are consistent with the notion that the major effects of FTS result from blocking of Ras activation. First, it is well documented that active Ras, operating via the Raf/MEK/ERK and the PI3-K/Akt/GSK-3 pathways, regulates the amounts of cyclin D1 and of CDK4/cyclin D1 assembly, leading to an increase in E2F transcriptional activity and enhanced cell proliferation (22). Indeed, we found that FTS induced a decrease in E2F-regulated genes. The apparent decreases observed in the expression of E2F-regulated genes, such as cyclin E2 and CDC2, provide an explanation for the FTS-induced inhibition of U87 cell growth. Second, studies have shown that the level and activity of HIF-1α protein are controlled by Ras (33). Ras regulates the stability and transcriptional activity of HIF-1α (33) by mechanisms that involve, respectively, GSK-3-dependent and ERK-dependent phosphorylation of the transcription factor (30). Our present finding that FTS inhibited ERK and Akt activation (Fig. 1) is consistent with the notion that Ras inhibition by FTS leads to inhibition of Ras signaling and destabilization of HIF-1α protein.

The strong association between Ras-HIF-1α and tumorigenicity is well documented. For example, active Ras increases HIF-1α expression in breast cancer cells (33), whereas expression of HIF-1α is blocked by a PI3-K inhibitor in prostate cancer cells (34) and in Ras-transformed NIH3T3 cells (35). Inhibition of ERK in HepG2 cells (36) and in colon cancer cells (37) resulted in blocking of HIF-1α activation or expression. In another study with NIH3T3 cells, ERK was shown to enhance HIF-1α transcriptional activity, whereas Akt was shown to stabilize HIF-1α protein (30). In addition, expression of a dominant-negative form of PI3-K or expression of PTEN resulted in a decrease in HIF-1α activity in U373 GBM cells (38). Related studies showed strong expression of HIF-1α in human gliomas (3, 39, 40) that exhibit high Ras-GTP levels and in pancreatic tumor cell lines (41) that harbor oncogenic Ras and/or overexpress *EGFR* (42). Our present results show that a reduction in active Ras in GBM (Fig. 1) is accompanied by a dramatic decrease in HIF-1α protein (Fig. 5). The proteasome inhibitor MG132 blocked the disappearance of HIF-1α in FTS-treated GBM cells. Thus, it seems that the decrease in HIF-1α is a result of enhanced degradation of the protein via the known mechanism of proteasomal HIF-1α degradation (43).

In this study we focused on the highly significant FTS-induced changes observed in HIF-1α-regulated genes in light of the critical role that this factor plays in maintenance of the malignant phenotype of GBM (3, 39, 40). HIF-1α regulates the expression of many enzymes that participate in glycolysis, a major energy pathway in GBM and in many other types of human tumors (44). We found that 12 genes of the glycolytic pathway (23, 24) were transcriptionally down-regulated by FTS in U87 cells (Fig. 4). This can explain the observed decrease in ATP production. The FTS-induced decrease in expression of both glycolytic enzymes and Glut-1 suggests not only that glycolysis was halted but also that glucose uptake was blocked.

We cannot tell from our experiments whether the FTS-induced death of U87 cells was attributable to the general energy crisis or to both the reduction in ATP and the activation of specific cell-death pathways. It was recently shown that down-regulation of HIF-1α by phosphorothioate antisense HIF-1α oligonucleotide causes apoptotic cell death in U87 cells (45). That study showed that the cytotoxic effect of the antisense HIF-1α was independent of p53 but could be attenuated by caspase inhibitors. We have not yet examined the effects of FTS on the apoptotic machinery in U87 cells, although we know that in other cells, for example, in rat intestinal epithelial cells, FTS promotes anoikis by a caspase-3-dependent mechanism (46). Thus, the observed FTS-induced decrease in HIF-1α protein in GBM cell lines and, taken together with the results of the above-mentioned study (45), suggest the possibility that FTS induces apoptotic cell death in U87 cells. Additional studies are required to resolve this question.

Finally, many studies have now pointed to HIF-1α as an important target for anticancer drugs. Our results provide evidence for the existence of a potent new down-regulator of HIF-1α, namely, the Ras inhibitor FTS. Additional studies are needed to determine whether this inhibitor is capable of blocking *in vivo* the HIF-1α-dependent invasiveness, survival, and angiogenesis of GBM.

Acknowledgments

Received 8/19/2004; revised 11/8/2004; accepted 11/19/2004.

Grant support: Jacqueline Seroussi Memorial Foundations for Cancer Research (Y. Kloog).

The costs of publication of this article were defrayed in part by the payment of page charges. This article must therefore be hereby marked advertisement in accordance with 18 U.S.C. Section 1734 solely to indicate this fact.

We thank the Arison-Dorsman family, Tel-Aviv, Israel, for their donation of DNA chips to Pediatric Oncology, Chaim Sheba Medical Center, and S.R. Smith for editorial assistance.

References

1. Holland EC. Gliomagenesis: genetic alterations and mouse models. Nat Rev Genet 2001;2:120–9.
2. Maher EA, Furnari FB, Bachoo RM, et al. Malignant glioma: genetics and biology of a grave matter. Genes Dev 2001;15:1311–33.
3. Korkolopoulou P, Patsouris E, Konstantinidou AE, et al. Hypoxia-inducible factor 1α/vascular endothelial growth factor axis in astrocytomas. Associations with microvessel morphometry, proliferation and prognosis. Neuropathol Appl Neurobiol 2004;30:267–78.
4. Li J, Yen C, Liaw D, et al. PTEN, a putative protein tyrosine phosphatase gene mutated in human brain, breast, and prostate cancer. Science 1997;275:1943–7.
5. Chakravarti A, Zhai G, Suzuki Y, et al. The prognostic significance of phosphatidylinositol 3-kinase pathway activation in human gliomas. J Clin Oncol 2004;22:1926–33.
6. Jiang BH, Aoki M, Zheng JZ, Li J, Vogt PK. Myogenic signaling of phosphatidylinositol 3-kinase requires the serine-threonine kinase Akt/protein kinase B. Proc Natl Acad Sci U S A 1999;96:2077–81.
7. Eldar-Finkelman H. Glycogen synthase kinase 3: an emerging therapeutic target. Trends Mol Med 2002;8:126–32.
8. Guha A, Dashner K, Black PM, Wagner JA, Stiles CD. Expression of PDGF and PDGF receptors in human astrocytoma operation specimens supports the existence of an autocrine loop. Int J Cancer 1995;60:168–73.
9. Shinojima N, Tada K, Shiraishi S, et al. Prognostic value of epidermal growth factor receptor in patients with glioblastoma multiforme. Cancer Res 2003;63:6962–70.
10. Shields JM, Pruitt K, McFall A, Shaub A, Der CJ. Understanding Ras: "it ain't over 'til it's over." Trends Cell Biol 2000;10:147–54.
11. Bos JL. Ras oncogenes in human cancer: a review. Cancer Res 1989;49:4682–9.
12. Downward J. Targeting RAS signalling pathways in cancer therapy. Nat Rev Cancer 2003;3:11–22.
13. Guha A, Feldkamp MM, Lau N, Boss G, Pawson A. Proliferation of human malignant astrocytomas is dependent on Ras activation. Oncogene 1997;15:2755–65.
14. Cox AD, Der CJ. Farnesyltransferase inhibitors: promises and realities. Curr Opin Pharmacol 2002;2:388–93.
15. Kloog Y, Cox AD, Sinensky M. Concepts in Ras-directed therapy. Expert Opin Investig Drugs 1999;8:2121–40.
16. Marciano D, Ben Baruch G, Marom M, Egozi Y, Haklai R, Kloog Y. Farnesyl derivatives of rigid carboxylic acids—inhibitors of ras-dependent cell growth. J Med Chem 1995;38:1267–72.
17. Elad-Sfadia G, Haklai R, Ballan E, Gabius HJ, Kloog Y. Galectin-1 augments Ras activation and diverts Ras

signals to Raf-1 at the expense of phosphoinositide 3-kinase. J Biol Chem 2002;277:37169–75.
18. Rotblat B, Niv H, Andre S, Kaltner H, Gabius HJ, Kloog Y. Galectin-1(L11A) predicted from a computed galectin-1 farnesyl-binding pocket selectively inhibits Ras-GTP. Cancer Res 2004;64:3112-8.
19. Eisen MB, Spellman PT, Brown PO, Botstein D. Cluster analysis and display of genome-wide expression patterns. Proc Natl Acad Sci U S A 1998;95:14863–8.
20. Dennis G Jr, Sherman BT, Hosack DA, et al. DAVID: database for annotation, visualization, and integrated discovery. Genome Biol 2003;4:P3.
21. Hosack DA, Dennis G Jr, Sherman BT, Lane HC, Lempicki RA. Identifying biological themes within lists of genes with EASE. Genome Biol 2003;4:R70.
22. Sherr CJ. D1 in G2. Cell Cycle 2002;1:36–8.
23. Harris AL. Hypoxia—a key regulatory factor in tumour growth. Nat Rev Cancer 2002;2:38–47.
24. Minchenko A, Leshchinsky I, Opentanova I, et al. Hypoxia-inducible factor-1-mediated expression of the 6-phosphofructo-2-kinase/fructose-2,6-bisphosphatase-3 (PFKFB3) gene. Its possible role in the Warburg effect. J Biol Chem 2002;277:6183–7.
25. Manalo DJ, Rowan A, Lavoie T, et al. Transcriptional regulation of vascular endothelial cell responses to hypoxia by HIF-1. Blood. Epub 16 Sept 2004.
26. El-Obeid A, Bongcam-Rudloff E, Sorby M, Ostman A, Nister M, Westermark B. Cell scattering and migration induced by autocrine transforming growth factor α in human glioma cells *in vitro*. Cancer Res 1997;57: 5598–604.
27. Miyazaki K, Kawamoto T, Tanimoto K, Nishiyama M, Honda H, Kato Y. Identification of functional hypoxia response elements in the promoter region of the DEC1 and DEC2 genes. J Biol Chem 2002;277:47014–21.
28. Boado RJ, Black KL, Pardridge WM. Gene expression of GLUT3 and GLUT1 glucose transporters in human brain tumors. Brain Res Mol Brain Res 1994;27:51–7.
29. Mateo J, Garcia-Lecea M, Cadenas S, Hernandez C, Moncada S. Regulation of hypoxia-inducible factor-1α by nitric oxide through mitochondria-dependent and -independent pathways. Biochem J 2003;376:537–44.
30. Sodhi A, Montaner S, Miyazaki H, Gutkind JS. MAPK and Akt act cooperatively but independently on hypoxia inducible factor-1α in rasV12 upregulation of VEGF. Biochem Biophys Res Commun 2001;287:292–300.
31. Feldkamp MM, Lau N, Rak J, Kerbel RS, Guha A. Normoxic and hypoxic regulation of vascular endothelial growth factor (VEGF) by astrocytoma cells is mediated by Ras. Int J Cancer 1999;81:118–24.
32. Woods SA, McGlade CJ, Guha A. Phosphatidylinositol 3′-kinase and MAPK/ERK kinase 1/2 differentially regulate expression of vascular endothelial growth factor in human malignant astrocytoma cells. Neuro-oncol 2002;4:242–52.
33. Blancher C, Moore JW, Robertson N, Harris AL. Effects of ras and von Hippel-Lindau (VHL) gene mutations on hypoxia-inducible factor (HIF)-1α, HIF-2α, and vascular endothelial growth factor expression and their regulation by the phosphatidylinositol 3′-kinase/Akt signaling pathway. Cancer Res 2001;61: 7349–55.
34. Gao N, Ding M, Zheng JZ, et al. Vanadate-induced expression of hypoxia-inducible factor 1α and vascular endothelial growth factor through phosphatidylinositol 3-kinase/Akt pathway and reactive oxygen species. J Biol Chem 2002;277:31963–71.
35. Mazure NM, Chen EY, Laderoute KR, Giaccia AJ. Induction of vascular endothelial growth factor by hypoxia is modulated by a phosphatidylinositol 3-kinase/Akt signaling pathway in Ha-*ras*-transformed cells through a hypoxia inducible factor-1 transcriptional element. Blood 1997;90:3322–31.
36. Mottet D, Michel G, Renard P, Ninane N, Raes M, Michiels C. Role of ERK and calcium in the hypoxia-induced activation of HIF-1. J Cell Physiol 2003;194: 30–44.
37. Fukuda R, Hirota K, Fan F, Jung YD, Ellis LM, Semenza GL. Insulin-like growth factor 1 induces hypoxia-inducible factor 1-mediated vascular endothelial growth factor expression, which is dependent on MAP kinase and phosphatidylinositol 3-kinase signaling in colon cancer cells. J Biol Chem 2002;277:38205–11.
38. Jiang BH, Jiang G, Zheng JZ, Lu Z, Hunter T, Vogt PK. Phosphatidylinositol 3-kinase signaling controls levels of hypoxia-inducible factor 1. Cell Growth Differ 2001;12:363–9.
39. Zagzag D, Friedlander DR, Margolis B, et al. Molecular events implicated in brain tumor angiogenesis and invasion. Pediatr Neurosurg 2000;33:49–55.
40. Vordermark D, Brown JM. Evaluation of hypoxia-inducible factor-1α (HIF-1α) as an intrinsic marker of tumor hypoxia in U87 MG human glioblastoma: *in vitro* and xenograft studies. Int J Radiat Oncol Biol Phys 2003;56:1184–93.
41. Akakura N, Kobayashi M, Horiuchi I, et al. Constitutive expression of hypoxia-inducible factor-1α renders pancreatic cancer cells resistant to apoptosis induced by hypoxia and nutrient deprivation. Cancer Res 2001;61:6548–54.
42. Korc M. Role of growth factors in pancreatic cancer. Surg Oncol Clin N Am 1998;7:25–41.
43. Huang LE, Gu J, Schau M, Bunn HF. Regulation of hypoxia-inducible factor 1α is mediated by an O_2-dependent degradation domain via the ubiquitin-proteasome pathway. Proc Natl Acad Sci U S A 1998;95:7987–92.
44. Seagroves TN, Ryan HE, Lu H, et al. Transcription factor HIF-1 is a necessary mediator of the Pasteur effect in mammalian cells. Mol Cell Biol 2001;21: 3436–44.
45. Dai S, Huang ML, Hsu CY, Chao KS. Inhibition of hypoxia inducible factor 1α causes oxygen-independent cytotoxicity and induces p53 independent apoptosis in glioblastoma cells. Int J Radiat Oncol Biol Phys 2003;55:1027–36.
46. Shalom-Feuerstein R, Lindenboim L, Stein R, Cox AD, Kloog Y. Restoration of sensitivity to anoikis in Ras-transformed rat intestinal epithelial cells by a Ras inhibitor. Cell Death Differ 2004;11:244–7.